*Research Journal of Engineering Sciences* ISSN 2278 – 9472
Vol. **6(11), 7**-19, December **(2017)** *Res. J. Engineering Sci.*

# Intensity - duration - frequency curves and hydrological response of retention ponds in the city of Lome (Togo, West Africa)

**Gbafa K.S.*[1], Tiem S.[1] and Kokou K.[2]**
[1]Ecole Nationale Supérieure d'Ingénieurs, Université de Lomé, Togo, West Africa
[2]Faculté Des Sciences, Université de Lomé, Togo, West Africa
gbafafelix@gmail.com

**Available online at: www.isca.in, www.isca.me**
Received 26th October 2017, revised 3rd December 2017, accepted 22th December 2017

## Abstract

*This study aims to contribute to the reduction of natural disaster risks related to floods in the city of Lome through modeling Intensity - Duration - Frequency (IDF) curves, and determining the storage threshold of retention ponds. 33 years of rainfall data were adjusted by the Log normal, Gumbel and GEV distributions. The Akaike (AIC) and Bayesian (BIC) criteria helped to determine the most suitable distribution laws. The quantiles of the return periods 5, 10; 20; 50 and 100 years are calculated and modeled based on the Montana, Talbot, Keifer-Chu and Wanieslita formulas. The parameters of retention basins were used to estimate their hydrological response based on the IDF curves established by applying the rational equation. Gumbel and Log normal laws fit the short duration rains well whereas GEV fit the medium and long duration rains better. The Keifer-Chu formula is most suitable for modeling IDF curves for the city of Lomeas it has the lowest mean squared error and the highest correlation coefficients. Regarding the hydrological response of detention basins, the results show a deficit of storage capacity. The threshold rains that fill each basin during the concentration time is less than a two (02) years return period rain.*

**Keywords:** Modeling, Extreme rains, hydrological response, returning ponds, Lomé, Togo.

## Introduction

Torrential rains and resulting floods are the most noticeable illustration of the impacts of extreme weather events. Sometimes, several African cities, just coming out of periods of drought, are subsequently faced with long periods of unprecedented flooding[1]. All African cities are to varying degrees vulnerable to floods and each adapts in its own way. The usual challenges are the lack of housing, energy, communication) disaster management, relief organization and infrastructure. West Africa has experienced increased flooding in recent years[2-5]. In 2007, 2.6 million people were affected by floods, which caused several deaths[2].

In Togo, about 60 urban and rural floods recorded between 1925 and 1992 caused material damage and loss of life[6]. In 2007, Togo recorded, in two of its administrative regions (maritime and Savane), the following flood related loses: 42 deaths, 245 869 victims, 51 902 destroyed homes, 31 care units, 1 176 classrooms,10,957 ha of crops land, and 23,061 head of cattle lost or damaged[7]. This damage is estimated at more than 23 billion CFA francs[8]. The situation worsened considerably in 2008 with the destruction of several bridges paralyzing all economic activity between Togo and the hinterland countries[9]. In Lomé, the same areas and populations are repeatedly affected every year, and new settlements and populations are becoming vulnerable to flooding[10]. The first factor involved in flood-related natural disasters is undoubtedly rainfall. Rainfall variability is generally expressed as mean maximum rainfall and as the frequency and intensity of extreme rainfall in a given region. Short-term extreme precipitation remains the main cause of the sudden and catastrophic floods that can occur in many small watersheds.

The effectiveness of the response to flood situations lies in the availability and performance of water and sanitation facilities. Indeed, the design of any hydraulic structure requires that the desired level of performance be specified[11]. According to these authors, the level of performance is often determined as a function of potential damage and the severity of the weather hazards that are likely to cause a break, a malfunction or the overflow of the structure in question. Thus, in the case of stormwater management infrastructure, the sizes of the various components of the system (pipelines, retention ponds, etc.) are established according to the return period of intense rainfall events[12-15]. This information is often expressed in the form of Intensity Time Frequency (IDF) curves obtained from a statistical study of extreme events recorded in a given territory[16]. These curves are at the basic of all design studies of storm water management infrastructure and they play a major role in the state of the art hydrological applications[17].

Unfortunately, very little research has been done on the establishment of IDF rainfall curves in tropical Africa. First, there are the old publications based on a methodology which is no longeradequate[18,19]. Other recent, studies published work on

IDF curves for stations located in the Congo[4,20]. In Togo, the only true previous study resulted in high- duration - frequency (HDF) curves for return periods 1; 2; 5; 10 and 20 years[21]. This study, previously used in the design of hydraulic structures, is outdated today and does not guarantee the safety of storm water management works in the current context of climate change. It's shown that a noticeable shortage of sanitation facilities in the city of Lome expressed by the high proportion of works done by the population , networks of gutters without outlets and the small number of retention ponds with gravity drain (11 of 36)[22]. These authors have also identified serious faults in the design of stormwater drainage works, especially retention ponds. This observation is confirmed by the Master Plan of Sanitation (PDA) for the city of Lome, which states that the normal tidal range between the minimum level (set by the water table) and the maximum level is less than one meter[23]. This situation requires not only the study of the level of service of retention basins in the city of Lome but also and especially, a detailed study of precipitation at the sub-hourly scale, because the process of stagnation of water does not arise only in terms of quantity but also in terms of rainfall intensity[24,25].

This article aims to contribute to the reduction of flood risk in the city of Lome. Specifically, it aims to i. model Intensity Duration Frequency (IDF) curves, and ii. determine the threshold intensities of effectiveness of retention ponds in the city of Lomé.

## Material and methods

**Study area:** The city of Lomé is located in the extreme south-west corner of Togo (Figure-1). It extends along the coast of the Gulf of Guinea westwards to the Ghana border. Lome is thus, a border town that covers an area of nearly 90 km² [26].

Lomé enjoys a Guinean subequatorial coastal climate characterized by two rainy seasons (March / April to July and September to November), and two dry seasons (in August then between November and February)[27,28.,29]. Lomé is the part of Togo with the lowest rainfall (800 to 900 mm of rain per year). The average humidity exceeds 75%. The average monthly minimum values range from 57-58% during the dry season and 71-73% during the rainy season[26,29]. The maximum average temperature is 30.7°C in the afternoon and the minimum 23.1 ° C in the morning. From south to north, the city consists of three physiographic zones[26,29]: i. Lower town: located between the sea and the lagoon, it is an ancient flat dune ridge with altitudes between 2 and 5.5 m above sea level. It is the historical heart of Lome. ii. The lagoon zone: located about 2.5 km from the seafront, in places it has a width of about 200 m. The lagoon zone is composed of an equilibrium channel and 3 lakes (West Lake, East Lake and Lake Bè). iii. Upper town: this is the plateau area to the north of the lagoon, rising to 35 m altitude. It is bounded in the northeast by the Zio River and in the west by the Ghana border[26].

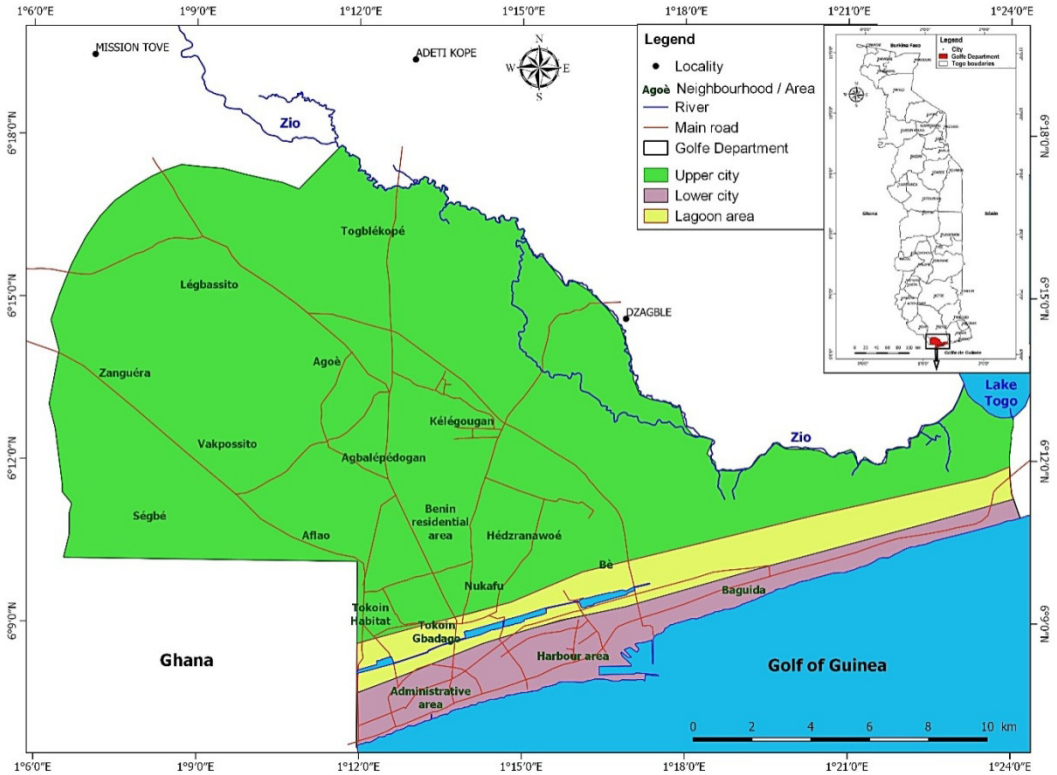


**Figure-1:** Study area.

**Collection of rainfall and hydrological data:** Most of the data used in this study comes from the records of the Lome airport synoptic station pluviographs[30]. This systematically analyzed data is available for the period 1965 to 1997 including more than 1515 rainy days. The raw data in Microsoft Excel format was calculated in Matlab version 99.491 environment and the results exported as Microsoft Excel data or JPEG graphics.

**Formatting and characterization of rainfall data:** Once the data counting completed, the statistical parameters for each rain period were calculated. These are: maximum, minimum, range, mode, median, mean, standard deviation and coefficient of variation.

**Probability distribution of the extreme values of each averse:** This is done to determine the law that best explains rainfall of given duration. The three most used distributions are applied for each shower. These are the Gumbel, the GEV and the Log normal distributions[31,32]. A theoretical justification for the application of these laws to the case of maximum annual values was given[33]. The Kendall stationarity test is used to detect trends in the series, and the Wald-Wolfowitz independence to verify, the existence of sequential dependency in the observations[34,35]. Criteria for the comparison of the statistical laws used are: the Akaike Criteria (AIC), and the Bayesian Criteria (BIC)[36]. The lower these criteria, the better the distribution law. The Kolmogorov-Smirnov test was performed in each case to verify the goodness of fit[37].

**Intensity duration frequency curves:** Let us symbolize the average intensity of rain by i (expressed in $mm.h^{-1}$), the aggregation time of rain by d (expressed in min) and the return period by T (expressed in years). The IDF relationship is then expressed mathematically by Equation 1. In general, rain intensity decreases with aggregation time and increases with return period, that is to say that the intensities weaken as duration lengthen[38]. This implies that the function i must be a decreasing function and therefore cannot be bell shaped. This property makes it possible to overcome without problem the jump between 2 and 24 h in the modeling of the IDF curves. Several IDF related models are selected for this study and are applied to the Lomé airport station data.

$$i = f(T, d) \quad (1)$$

**The Montana formula:** This is one of the most popular models used in the field because of its simplicity [39]. The model is expressed for a return time T by Equation-2.

$$i_T(t) = at^{-b} \quad (2)$$

**The Talbot Formula:** This model is recommended in the standards of Swiss road professionals[39]. The model for a given return time T is expressed by Equation-3.

$$i_T(t) = \frac{a}{b+t} \quad (3)$$

**The Keifer-Chu formula:** This is similar to the Talbot model except that it is more robust because of the introduction of a third parameter giving Equation-4 [40].

$$i_T(t) = \frac{a}{(b+t)^c} \quad (4)$$

**The Wanieslita formula:** This simplified general Equation combines the other three models[41]. Unlike the other Equations it allows all the curves to be drawn using a single formula given in Equation-5:

$$i(t) = \frac{aT^b}{(c+t)^e} \quad (5)$$

The parameters a, b, c and e are numerical coefficients that depend on frequency (or the return period T), the measurement site and rainfall duration.

**The best IDF model:** Having specified the different IDF models, it is necessary to ensure their effectiveness comparing them to find the best one for Lome. To do this, two criteria were used. The mean squared error (MSE) and the correlation coefficient (R). These statistical indicators were calculated for each model. The correlation coefficient R appreciates the linear relation between the theoretical model and actual data. It lies between -1 and 1.The mean square error (MSE) is used to compare multiple adjustments and to determine the best model with the lowest error.

**Hydrological response of retention basins to rainfall:** For the analysis of the efficiency of the sanitation works, only the built retention ponds were studied. Unbuilt depressions that function as storm water storage areas were not considered. The hydrological data (surfaces A and runoff coefficients C and concentration time Tc of basins, capacity V and infiltration coefficients of basins) are obtained from the Hydraulics Head Office (DGH) in Lome. The flow drained by each basin was calculated and the retention threshold of the basins were estimated.

The flow Q (m3 / s) runoff on a catchment area (A in ha), and runoff coefficient C during a rain of intensity (I in l / s) is expressed by Equation-6 of the rational formula. In this equation, μ represents the unit conversion coefficient.

$$Q = \mu . C . I . A \quad (6)$$

The retention threshold of a basin is the intensity of rain which for a duration equal to the concentration time causes the filling of the corresponding retention basin. This relation is represented by Equation-7. By incorporating Equation-6 in the latter one obtains 8.

$$V = Q . Tc \quad (7)$$

The volumes discharged by gravity or pumping during a time equal to the concentration time of the contributing watershed is taken into account in the calculations.

$$Is = \frac{\mu V}{C.A.Tc} \quad (8)$$

The comparison of threshold intensity (Is) and theoretical intensities per return period makes it possible to know if the retention pond is effective or not. To achieve this, the threshold intensities are calculated for durations equal to the concentration time of each basin and compared with those corresponding to the IDF model used for the city of Lomé for return periods of less than 20 years. These return periods are indeed the most used in urban hydrology for the design of hydraulic structures[42].

## Results and discussion

**Characteristics of rainfall data:** Statistical parameters calculated for each rain duration show that rainfall intensities decrease as duration increases (Table-1). For the two extreme rain periods (5 minutes and 120 minutes), the maximum average intensities are 5 mm/min and0.7 mm / min and the minimum mean intensities are 1.6 mm / min at 0.1 mm / min. (Table-1). The average values are 2.4970 ± 0.7535 mm / min and 0.3094 ± 0.1279 mm/min for the same rain periods (Table-1). With regard to the most frequent values, the modes range from 2 to 0.4 mm/min for rain periods of 5 to 120 min. The most frequent values of intensity are higher than the average values for rainfall 5 to 25 min and lower than the mean rainfalls 30 to 120 min. The standard deviation, which is a parameter indicating the dispersion of the values, varies from 0.7535 to 0.1279 for rains of 5 to 120 min. Intensity values are more grouped for long-duration rainfall than for short periods.

**Adjustment of the distribution laws:** The probability distributions of the extreme values show a good fit of the observed data to the Gumbel, the GEV and the Log normal distributions (P> 0.05). But the results show that the distribution laws studied do not fit the observed data in the same way. It is thus found that for 5-min rain of only (Figure-2), the three laws seem to describe the data best. For rain adjustment of 35 min rain (Figure-3). The observation is different. Indeed, for this case, the Lognormal and Gumbel laws diverge from real data. This divergence is more marked at the tail of the distribution.

**Table-1:** StatisticalCaractéristics of rainfull in Lome.

| Rain full duration | Maxi. | Mini. | stretch | Mode | Median | average | Standard. deviation | Coef. of variation |
|---|---|---|---|---|---|---|---|---|
| 5 min | 5.0 | 1.6 | 3.4 | 2.0 | 2.4 | 2.4970 | 0.7535 | 0.3018 |
| 10 min | 3.9 | 1.3 | 2.6 | 1.8 | 1.9 | 2.0667 | 0.5824 | 0.2818 |
| 15 min | 3.1 | 1.1 | 2.0 | 1.7 | 1.7 | 1.8061 | 0.4520 | 0.2503 |
| 20 min | 2.4 | 1.0 | 1.4 | 1.7 | 1.6 | 1.6091 | 0.3311 | 0.2057 |
| 25 min | 2.0 | 0.4 | 1.6 | 1.5 | 1.4 | 1.4273 | 0.3145 | 0.2204 |
| 30 min | 1.7 | 0.4 | 1.3 | 1.4 | 1.3 | 1.2909 | 0.2765 | 0.2142 |
| 35 min | 1.5 | 0.3 | 1.2 | 1.1 | 1.2 | 1.1394 | 0.2384 | 0.2092 |
| 40 min | 1.3 | 0.3 | 1.0 | 1.1 | 1.1 | 1.0394 | 0.2135 | 0.2054 |
| 45 min | 1.3 | 0.3 | 1.0 | 1.0 | 1.0 | 0.9485 | 0.1856 | 0.1957 |
| 50 min | 1.2 | 0.3 | 0.9 | 0.9 | 0.9 | 0.8576 | 0.1768 | 0.2062 |
| 55 min | 1.2 | 0.3 | 0.9 | 0.9 | 0.8 | 0.7758 | 0.1871 | 0.2412 |
| 60 min | 1.1 | 0.3 | 0.8 | 0.8 | 0.7 | 0.7000 | 0.1696 | 0.2422 |
| 65 min | 1.1 | 0.2 | 0.9 | 0.6 | 0.6 | 0.6394 | 0.1713 | 0.2679 |
| 70 min | 1.0 | 0.2 | 0.8 | 0.6 | 0.6 | 0.5939 | 0.1619 | 0.2726 |
| 75 min | 1.0 | 0.2 | 0.8 | 0.6 | 0.6 | 0.5606 | 0.1580 | 0.2818 |
| 80 min | 0.9 | 0.2 | 0.7 | 0.6 | 0.5 | 0.5242 | 0.1480 | 0.2822 |
| 85 min | 0.9 | 0.2 | 0.7 | 0.6 | 0.5 | 0.5030 | 0.1489 | 0.2961 |
| 90 min | 0.8 | 0.2 | 0.6 | 0.5 | 0.5 | 0.4515 | 0.1228 | 0.2719 |
| 95 min | 0.8 | 0.2 | 0.6 | 0.4 | 0.4 | 0.4063 | 0.1268 | 0.3122 |
| 100 min | 0.8 | 0.2 | 0.6 | 0.4 | 0.4 | 0.3938 | 0.1268 | 0.3221 |
| 105 min | 0.8 | 0.2 | 0.6 | 0.4 | 0.4 | 0.3844 | 0.1247 | 0.3245 |
| 110 min | 0.8 | 0.1 | 0.7 | 0.4 | 0.4 | 0.3594 | 0.1241 | 0.3452 |
| 115 min | 0.7 | 0.1 | 0.6 | 0.4 | 0.3 | 0.3281 | 0.1198 | 0.3650 |
| 120 min | 0.7 | 0.1 | 0.6 | 0.4 | 0.3 | 0.3094 | 0.1279 | 0.4134 |

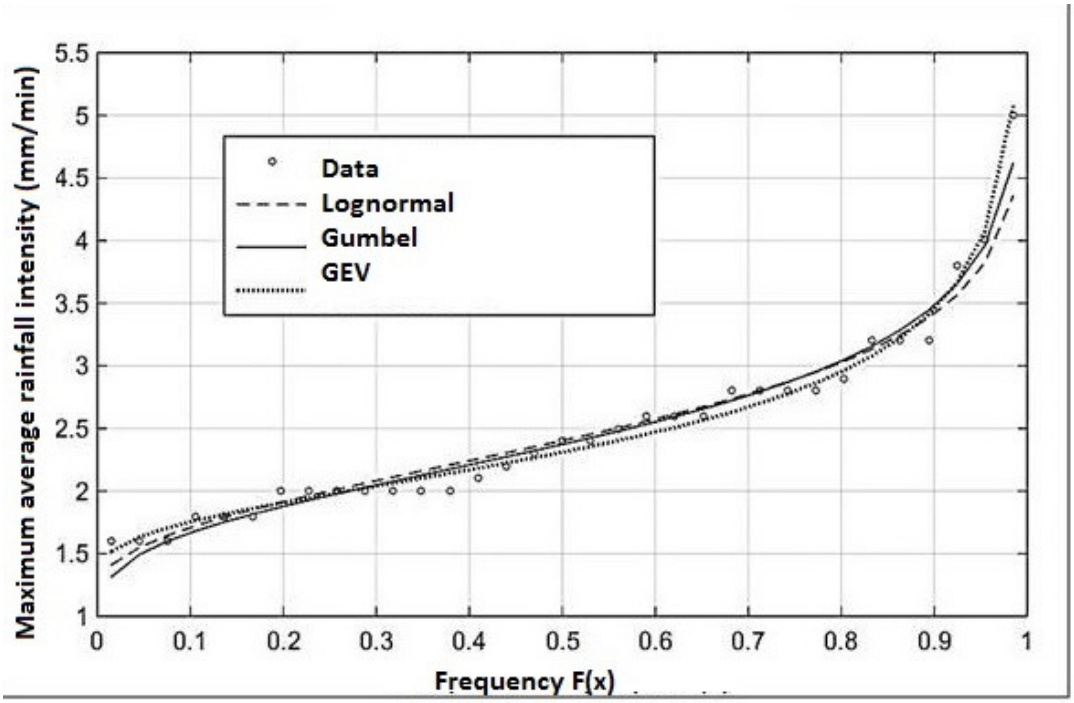


**Figure-2:** Maximum average 5min duration rainfall fit.

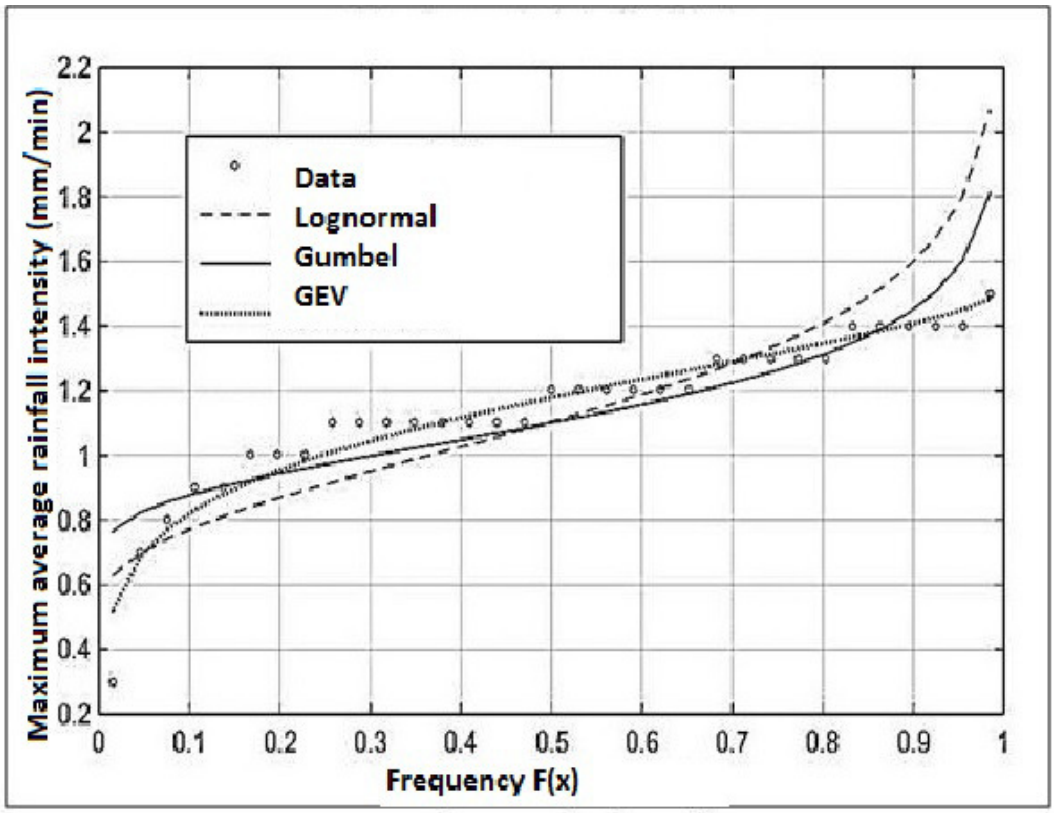


**Figure-3:** Maximum average 35 min duration rainfall fit.

With regard to the quality of the models, the results show that: i. The Gumbel law is the most suitable for describing rainfall of 5 to 15 min. ii. The log normal law is best suited for describing rainfall of 20; 25 and 40 min. iii. The GEV law is the most suitable for describing the maximum average rainfall intensities of 30 and 35 min, 45 to 120 min (Figure-4, 5 and Table-2).

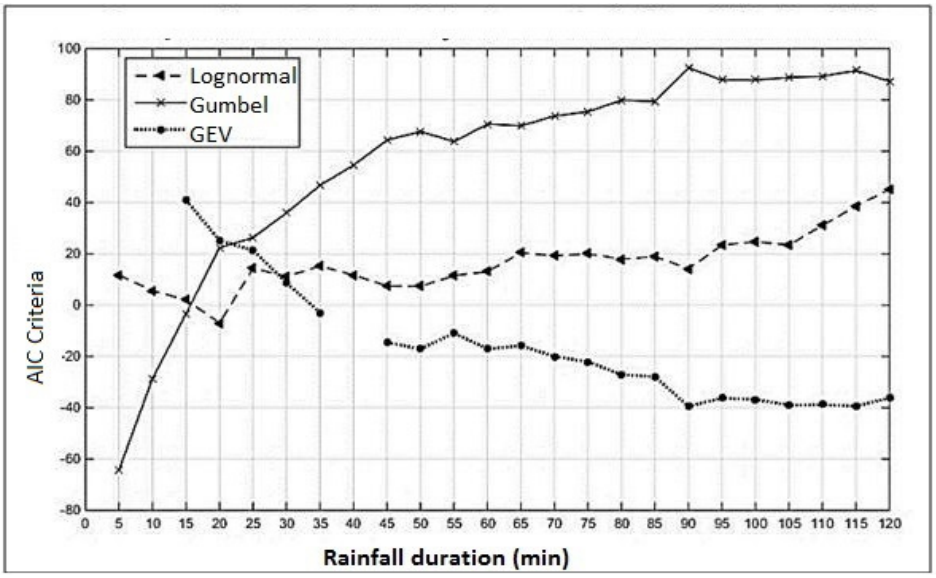


**Figure-4:** Comparison of adjustment laws based on AIC criteria.

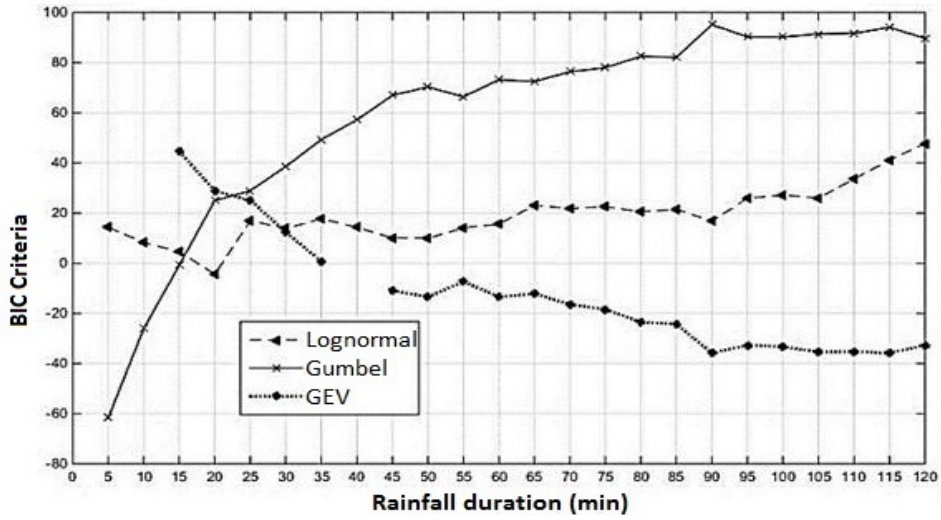


**Figure-4:** Comparison of adjustment laws based on BIC criteria.

**IDF model curves for the city of Lomé:** Knowing that the numerical coefficients (a, b, c and e) depend on the return period T and the duration of the rains, the models give different results. For the Montana model, parameters (a, b) increase with return period. They respectively lie from 8.12 to 14.04 and 0.54 to 0.61 (Table-3). For the Talbot formula, the first (a) increases from 66.93 to 82.19 and the second (b) decreases from 16.59 to 11.57. The three parameters (a, b, c) of the Keifer-Chu formula decrease as return period increases. Parameter a, from 1301.00 to 128.60, parameter b from 41.24 to 14.62 and parameter c. from 1.585 to 1.097.

**The best IDF model:** The modeled IDF curves give different results according to the type of model used and according to return period. This difference is reflected in mean squared errors (MSE) and correlation coefficients (R). The analysis of R values shows that they range from 0.973 to 0.998 for all the models fitted (Table-4). Therefore, all the models have a strong linear correlation with the real quantiles if one is interested in linear dependence between the models and the real quantiles.

With regard to the quality of the models, the results also show that the R of the Montana model is relatively low, compared to the other models regardless of the return time. For this model, the coefficient ranges from 0.972 to 0.975. On the other hand, the Montana model has a higher mean squared error, regardless of return period (Table-2), and is therefore less efficient compared to the other models. These errors range from 0.035 to 0.063. Of the remaining three models (Talbot, Keifer-Chu and Wanieslita), the Keifer-Chu model has the lowest mean squared errors and the highest correlation coefficient. This model is therefore selected as the best (Figure-4 and Table-5).

**Table-2:** Classification of distributions.

| Rain full duration (min) | Classification of distributions | | |
|---|---|---|---|
| | N°1 | N°2 | N°3 |
| 5 | Gumbel | Log-normal | -------- |
| 10 | Gumbel | Log-normal | -------- |
| 15 | Gumbel | Log-normal | GEV |
| 20 | Log-normal | Gumbel | GEV |
| 25 | Log-normal | GEV | Gumbel |
| 30 | GEV | Log-normal | Gumbel |
| 35 | GEV | Log-normal | Gumbel |
| 40 | Log-normal | Gumbel | -------- |
| 45 upto 120 | GEV | Log-normal | Gumbel |

**Table-3:** IDF model parameters.

| Formula | Return period | a | b | c | E |
|---|---|---|---|---|---|
| Montana | 5 | 8.1150 | 0.5392 | - | - |
| | 10 | 9.4130 | 0.5525 | - | - |
| | 20 | 10.7400 | 0.5667 | - | - |
| | 50 | 12.5800 | 0.5862 | - | - |
| | 100 | 14.0400 | 0.6008 | - | - |
| Talbot | 5 | 66.9300 | 16.5900 | - | - |
| | 10 | 71.9700 | 15.3500 | - | - |
| | 20 | 75.7600 | 14.1100 | - | - |
| | 50 | 79.6900 | 12.5900 | - | - |
| | 100 | 82.1900 | 11.5700 | - | - |
| Keifer-Chu | 5 | 1301.00 | 41.24 | 1.585 | - |
| | 10 | 358.60 | 28.15 | 1.326 | - |
| | 20 | 196.50 | 21.35 | 1.198 | - |
| | 50 | 139.80 | 16.60 | 1.120 | - |
| | 100 | 128.60 | 14.62 | 1.097 | - |
| Wanieslita | - | 137.3000 | 0.1374 | 21.640 | 1.217 |

**Table-4:** Comparison of models.

| Return period | Model | MSE | R |
|---|---|---|---|
| 10 years | Montana | 0.0353 | 0.9727 |
| | Talbot | 0.0040 | 0.9971 |
| | Keifer-Chu | 0.0020 | 0.9984 |
| | Wanieslita | 0.0052 | 0.9978 |
| 20 years | Montana | 0.0399 | 0.9752 |
| | Talbot | 0.0063 | 0.9961 |
| | Keifer-Chu | 0.0051 | 0.9967 |
| | Wanieslita | 0.0069 | 0.9967 |
| 50 years | Montana | 0.0507 | 0.9755 |
| | Talbot | 0.0138 | 0.9932 |
| | Keifer-Chu | 0.0131 | 0.9935 |
| | Wanieslita | 0.0146 | 0.9929 |
| 100 years | Montana | 0.0633 | 0.9743 |
| | Talbot | 0.0230 | 0.9904 |
| | Keifer-Chu | 0.0225 | 0.9907 |
| | Wanieslita | 0.0301 | 0.9891 |

**Table-5:** Keifer-Chu model parameters.

| Parameters | 2 years | 5 years | 10 years | 20 years | 50 years | 100 years |
|---|---|---|---|---|---|---|
| a | $2.171\ 10^5$ | 1301.0 | 358.600 | 196.500 | 139.800 | 128.600 |
| b | 87.760 | 41.240 | 28.150 | 21.350 | 16.600 | 14.620 |
| c | 2.527 | 1.585 | 1.326 | 1.198 | 1.120 | 1.095 |

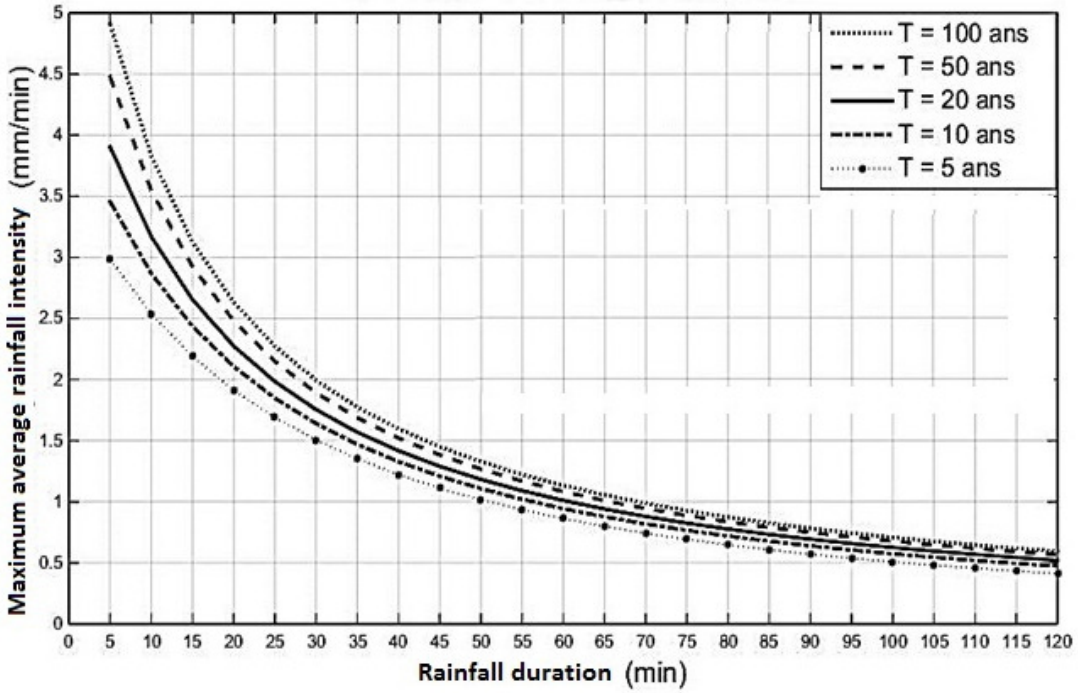


**Figure-5:** IDF curves for Lome.

This three-parameter model has one more parameter than the Talbot and Montana models and it is the most suitable for modeling IDF curves for the city of Lomé. The Wanieslita model, with four parameters (one more than Keifer-Chu model), comes only in third position in the classification. This is because for the other three models the parameters are calculated for each return period, unlike the Wanieslita model, which sets all four parameters once, regardless of the return period. This model then introduces more errors into the modeling of IDF curves.

**Characteristics of hydrological data:** A total of 23 retention ponds have been studied out of 38 in the city of Lome. Their runoff coefficients vary between 0.30 and 0.45 and the concentration times between 13.75 and 56 minutes (Table-5). Their run-off surfaces and retained volumes vary between 22 ha and 704 ha and 1800 $m^3$ with 100000 $m^3$ respectively.

**Table-6:** Characteristics of retention ponds[23].

| Retention Pond n° | Rundown Surface (Ha) | Runoff Coefficient C* | Concentration Time (min) | Retained Volume (m3) |
|---|---|---|---|---|
| R. Pond 1.1 | 65 | 0,35 | 34,64 | 4 800,00 |
| R. Pond 1.2 | 327 | 0,32 | 38,16 | 45 000,00 |
| R. Pond 2.1 | 141 | 0,35 | 56,00 | 29 107,00 |
| R. Pond 2.1' | 142 | 0,35 | 56,00 | 20 865,00 |
| R. Pond 2.2 | 72 | 0,35 | 33,63 | 9 564,00 |
| R. Pond 2.4 | 114 | 0,35 | 13,75 | 13 724,00 |
| R. Pond 2.5 | 36 | 0,35 | 14,30 | 5 600,00 |
| R. Pond 2.7 | 323 | 0,42 | 15,69 | 40 000,00 |
| R. Pond 2.7' | 362 | 0,43 | 15,69 | 78 000,00 |
| R. Pond 3.1 | 316 | 0,30 | 45,86 | 42 000,00 |
| R. Pond 3.3 | 345 | 0,30 | 33,10 | 75 000,00 |
| R. Pond 4.1 | 22 | 0,35 | 23,26 | 2 400,00 |
| R. Pond 4.2 | 249 | 0,40 | 19,26 | 37 000,00 |
| R. Pond 4.4 | 160 | 0,45 | 28,54 | 33 000,00 |
| R. Pond 4.6 | 22 | 0,45 | 15,12 | 1 800,00 |
| R. Pond 5.3 | 131 | 0,40 | 17,81 | 8 000,00 |
| R. Pond 5.4 | 108 | 0,35 | 45,61 | 10 000,00 |
| R. Pond 7.7 | 688 | 0,35 | 38,54 | 100 000,00 |
| R. Pond 7.8 | 465 | 0,35 | 28,09 | 40 000,00 |
| R. Pond 8.1 | 704 | 0,35 | 54,46 | 60 000,00 |
| R. Pond 9.1 | 252 | 0,35 | 58,14 | 10 000,00 |
| R. Pond 9.2 | 114 | 0,35 | 19,03 | 5 000,00 |
| R. Pond 9.7 | 32 | 0,35 | 22,51 | 2 000,00 |

**Containment ponds storage threshold:** The results show that for rainfall simulations of initially empty retention basins, the threshold intensities of only four (04) retention basins (R. P 2.1, R. P, 2.5, R. P 2.7' and R. P 3.3), exceed the 10-year rainfall. Five (05) retention basins have threshold intensities between the rains of two (02) and five (05) years and three (03) retention basins have threshold intensities between the rains of five (05) years and ten (10) year rains. Half of the retention ponds (11 out of 23) have threshold intensities less than two (02) years of rainfall (Figure-5).

The pools overflow with each rain. However, when the retention pond is half empty before the onset of rain, all threshold intensities are lower than the 2-year return rainfall (Figure-6). Generally these basins are half full even at the end of the rainy season with a few exceptions.

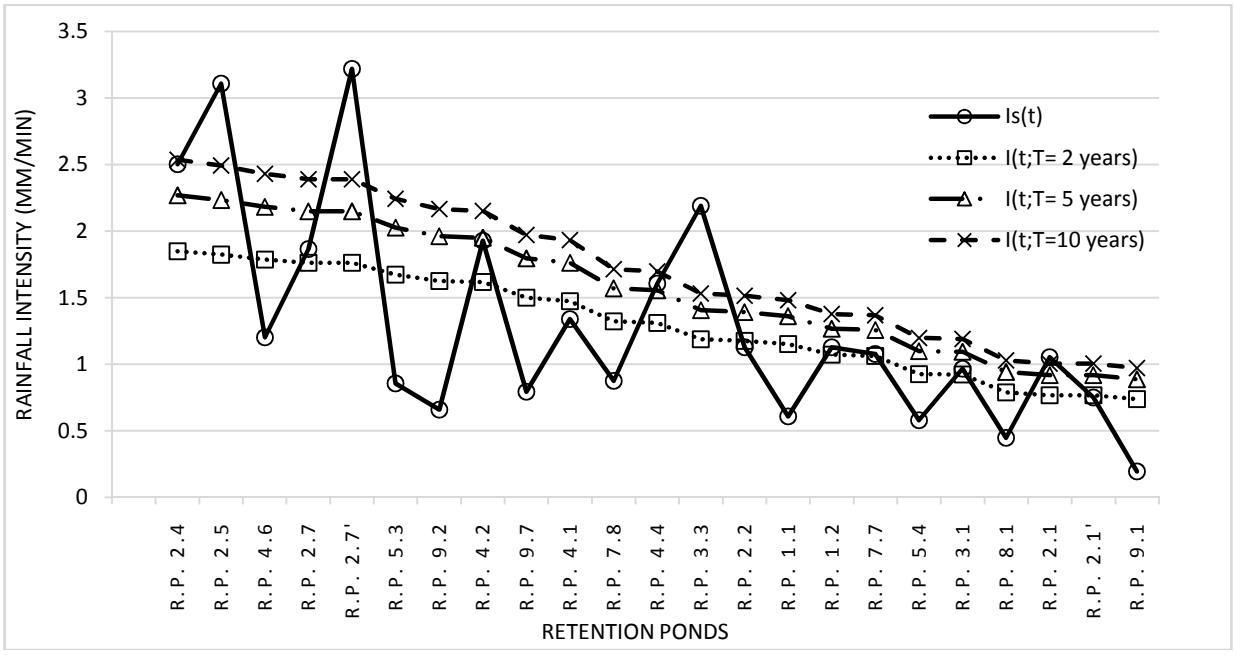


**Figure-5:** Comparison of threshold intensities with those of the model for empty retention basins.

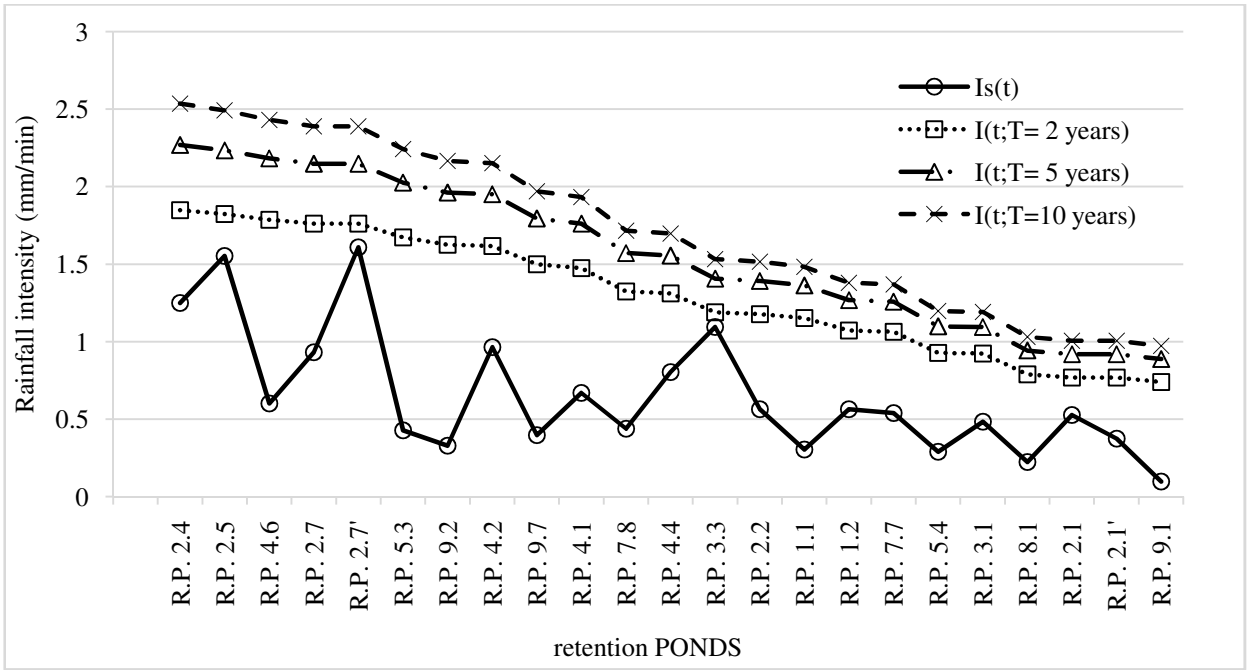


**Figure-6:** Comparison of threshold intensities with those of the half-empty reservoir model.

**Discussion: Choice of statistical distribution laws for rainfall intensity:** This study has determined the distribution law that best describes rainfall in the city of Lome. The results show that a single frequency model can best describe all the data sets of a meteorological station. In the present study, the results reveal that the Gumbel and Log normal laws fit the maximum average intensities of short-term rainfall and the GEV law fits those of medium and long durations in the city of Lome. This result is consistent with that obtained for the city of Abidjanwhenit was possible to use the three statistical laws (Lognormal, GEV and Gumbel) to describe annual maximum intensities[43]. Another study also shown that the probability distributions of maximum annual daily rainfall do not specifically obey a given rainfall regime[44]. According to these authors, in each climatic zone, there are at least three types of probability laws each having at least one zone of validity. This situation justifies the need to use several functions to find the most suitable for each station. These results further reaffirm the complexity of the analysis of average maximum rainfall intensities and confirm the observation already made by several previous studies[14,43,44]. Indeed, several studies have arrived at the conclusion as to the suitability of the distribution laws used. The probability distribution of two-component extreme values have been used tow[17,45]. With the aim of constructing IDF curves in the analysis of extreme events same studies used the Gumbel distribution[20, 44,47]. Other authors used the Log-normal distribution function because it fitted data better than the Gumbel distribution[43,48]. The Gumbel distribution seriously underestimates the values of large return periods[31,46,49]. After analyzing the longest and most reliable records of 169 rainfall stations it was demonstrated with theoretical and empirical arguments that the Gumbel distribution is not applicable to hydrological extremes[46].

**IDF curves and hydrological response of the urban basin:** The results of the IDF curves show that the Montana model is less efficient compared to the other models because it has the highest mean squared error and the lowest correlation coefficient. These results are confirmed when studying rainfall in Yangambi, Congo, authors obtained a quadratic error of 18%[14]. According to these previous authors, the Montana model did not satisfy the asymptotic constraint required when duration tends to zero. This is because this model corresponds to a series of parallel lines while the IDF law underlying the empirical quantiles has a curvature[38]. Therefore the so-called Montana formula cannot be used for aggregation times less than one day. Several previous studies simply advocate rejection of the Montana model[43, 44].

The comparison of the IDF curves obtained in the present study with the existing curves modeled for the 10-year return period, (period common to both works) shows that the old IDF curves (those obtained in 2003) overestimate the rainfall phenomenon for rainy periods between 5 to 15 min and 70 to 120 min[30]. This overestimation is more pronounced for very short rains (5 and 10 min). Several reasons could explain the difference observed between the IDF curves of the two works. First, the use of a single distribution law (Gibrat-Galton) by graphical adjustment on paper[30]. This methodology used to obtain the old curves does not make it possible to determine with precision the IDF quintiles. The differences between the curves are also due to the use of the Montana model (considered less suitable for modeling the Lomé curves compared to the other three models used (Talbot, Keifer-Chu and Wanieslita) without computer software for determining the old curves parameters.

Regarding the efficiency of the retention ponds in terms of rainwater management, rainfall simulations of these pools showed that for most of the basins studied the retention threshold intensities were lower than the return rainfall of 2 years. The ponds generally overflow with each rain. The threshold intensities obtained reveal some of the problems of sizing sanitation structures, particularly in the Togolese capital but also in other Togolese cities. The proportion of retention basins with gravity drain (11 out of the 36 in the city) assisted by the presence of pumping equipment on the retention ponds proves not only insufficiency of storage capacity but also a serious design fault. This observation is confirmed by the Master Plan of Sanitation in force in the city of Lomé, which states that the normal tidal range between the minimum level (set by the water table) and the maximum level is less than one meter[10,23]. Estimating the hydrological response of an urban basin in the city of Annaba in Algeria, authors obtained similar results[50]. These authors have obtained a peak flow on the urban watershed that exceeds the capacity of the existing stormwater drainage structure. These authors attribute this result to the effect of urbanization on the hydrological response of the watershed. As a result of urbanization, the response time of a watershed decreases considerably and peak flows increase[51]. In the local context, the urbanization of the basin can also be the cause of frequent floods.

## Conclusion

The present study modeled the IDF curves for the city of Lome allowing designers to determine the required rains for the optimal sizing of the hydraulic sanitation structures in order to contribute to the reduction of flood risk of in the city of Lome. Based on the mean squared error and correlation coefficients, we find the best IDF model in the Keifer-Chu formula, the model on which the new IDF curves were selected. This work advocates the Wanieslita, Talbot and Keifer-Chu type formulas but reject Montana formulations. The present work also demonstrated through the estimation of the response of the existing sanitation facilities a deficiency in the storage capacity of retention ponds.

## Références

**1.** Cheikh O.S., Ahmed M., Ozer P. and Ozer A. (2007). Risques d'inondation dans la ville de Nouakchott (Mauritanie). *Geo-Eco-Trop*, 31, 19-42.

**2.** Wade S., Faye S., Dieng M., Kaba M. and Kane N.R. (2009). Télédétection des catastrophes d'inondation urbaine: Le cas de la région de Dakar (Sénégal). *Journal d'Animation Scientifique,* 7.

**3.** Klassou K.S. (2011). L'urbanisation et l'assainissement pluvial au Togo. *Revue de géographie tropicale de l'environnement*, Abidjan, 45-60.

**4.** Sighomnou D., Tanimoun B., Alio A., Zomodo L., Ilia A., Olomoda I., Coulibaly B., Koné S., Zinsou D. and Dessouassi R. (2012). Crue exceptionnelle et inondation au cours des mois d'août et septembre 2012 dans le Niger moyen et inférieur. ABN, Niamey, 11.

**5.** Commission Economique des nations unies pour l'Afrique (2015). Rapport d'évaluation sur l'intégration et la mise en œuvre des mesures de réduction des risques de catastrophe au Togo, AddisAbaba, 76.

**6.** Sodogas A.V. and Gomado K. (2006). Analyse situationnelle des risques et facteurs de risques potentiels en matière de désastres au Togo.

**7.** PANA (2008). Plan d'action national d'adaptation aux changements climatiques. 113.

**8.** UNFCCC (2010). Communication nationale initiale du Togo sur les changements climatiques. Lomé: Presse de l'université de Lomé.

**9.** Gbafa S.K. (2010). Impacts de la réduction du niveau de service des infrastructures routières: Cas du pont de LANGABOU sur la RN 1 au Togo. Mémoire de DEA, Université de Lomé.

**10.** Klassou K.S. (2014). L'influence humaine dans l'origine et la gravité des inondations au Togo : cas de l'aménagement de l'espace dans la grande banlieue nord de Lomé (Togle-Adetikope). *Revue de géographie tropicale de l'environnement*, Abidjan, 2, 3-15.

**11.** Kingumbi A. and Mailhot A. (2010). Courbes Intensité–Durée–Fréquence (IDF): comparaison des estimateurs des durées partielles et des maximums annuels. *Hydrological Sciences Journal–Journal des Sciences Hydrologiques*, 55(2), 162-176.

**12.** Bourrier R. (1981). Les réseaux d'assainissement: calculs, applications et perspectives. *Technique et Documentation,* Paris, France.

**13.** Mailhot A., Rivard G., Duchesne S. and Villeneuve J.P. (2007). Impacts et adaptations liés aux changements climatiques en matière de drainage urbain au Québec. *Rapport no. R-874. INRS-ETE. Québec. Canada.*

**14.** Mohymont B. and Demarée G.R. (2006). Courbes intensité durée fréquence des précipitations à Yangambi Congo, au moyen de différents modèles de type Montana. *Hydrological Sciences–Journal–des Sciences Hydrologiques,* 51(2), 236-253.

**15.** Segond M.L., Neokleous N., Makropoulos C., Onof C. and Maksimovic C. (2007). Simulation and spatio-temporaldisaggregationof multi-site rainfall data for urban drainage applications. *Hydrol. Sci. J*., 52(5), 917-935.

**16.** Hogg W.D. and Carr D.A. (1985). Rainfall Frequency Atlas for Canada. Environnement Canada, *Atmospheric Environment Service*.

**17.** Willems P. (2000). Compound intensity/duration/frequency-relationship of extreme precipitation for two seasons and two storm types. *J hydrol*., 233, 189-205.

**18.** Bultot F. (1956). Etude statistique des pluies intenses en un point et sur une aire au Congo Belge et au Ruanda-Urundi. Publication de l'Institut National pour l'Etude Agronomique du Congo Belge. Communication no. 11. Bureau Climatologique. Bruxelles.

**19.** Pire J., Berruex M. and Quoidbach J. (1960). L'intensité des pluies au Congo et au Ruanda-Urundi. Mémoires-Collection in-4°. Livre VI. Fascicule 1. Classe des Sciences Techniques. Académie Royale des Sciences d'Outre-Mer.

**20.** Mohymont B., Demarée G.R. and Faka D.N. (2004). Establishment of IDF-curves for precipitation in the tropical area of Central Africa-comparison of techniques and results. *Natural Hazards and Earth System Sciences*, 4, 375-387.

**21.** CIEH (1984). Etude des pluies journalières de fréquence rare dans les pays membres du CIEH. Rapport de synthèse, 58.

**22.** Gbafa K.S., Tiem S. and Kokou K. (2017). Characterization of rainwater drainage infrastructure in the city of Lomé (Togo, West Africa). *European Scientific-Journal,* 13(30), 478-496.

**23.** DGH (2004). Plan Directeur d'Assainissement de la ville de Lomé. Rapport définitif, 286.

**24.** Van Tuu N., Lemoine B. and Pouplard J. (1981). Hydraulique routière. République française, *Ministère de la coopération et du développement*.

**25.** Wallez L. (2010). Inondations dans les villes d'Afrique de l'ouest: diagnostic et éléments de renforcement des capacités d'adaptation dans le Grand Cotonou. *Maîtrise en Environnement, Université de Sherbrooke, Sherbrooke*.

**26.** Adjoussi P. (2008). Vulnérabilité des systèmes côtiers à l'élévation du niveau marin entre la Volta et le Mono dans le golfe du Bénin (Afrique de l'Ouest). Thèse de doctorat d'Université. Université de Lomé, 416.

**27.** Aubréville A. (1937). Les forêts du Dahomey et du Togo. *Bulletin du Comité d'études historiques,* 29, 1-113.

**28.** Edjame K.S. (1992). Changement Climatique global : Les syndromes perçus au Togo. in Actes des journées Scientifiques de l'U.B., Presse De l'U.B. Lomé, 169-180.

**29.** Adjoussi P. (2000). Changement climatique global: Evaluation de l'évolution des parametres climatiques au Togo. Lomé: Université de Lomé FLESH.

**30.** Binguitcha-Fare K. (2003). Analyse des averses au Togo. Nouvelles édition africaines. Lomé

**31.** Wilks D.S. (1993). Comparison of three-parameter probability distributions for representing annual extreme and partial duration precipitation series. *Water Resource. Res.,* 29(10), 3543-3549.

**32.** Goula B.T., Brou K., Brou T., Savane I., Vamoryba F. and Bernard S. (2007). Estimation des pluies exceptionnelles journalières en zone tropicale: cas de la Côte d'Ivoire par comparaison des lois Log-normale et de Gumbel. *Hydrological Sciences–Journal– des Sciences Hydrologiques,* 52(1), 49-67.

**33.** Beirlant J., Vynckier P. and Teugels J.L. (1996). Excess functions and estimation of the extreme-value index. *Bernoulli*, 293-318.

**34.** Yue S. and Pilon P. (2004). A comparison of the power of the test, Mann-Kendall and bootstrap tests for trend detection/Unecomparaison de la puissance des tests t de Student, de Mann-Kendall et du bootstrap pour la détection de tendance. *Hydrological Sciences Journal*, 49(1), 21-37.

**35.** Haché M., Perreault L., Rémillard L. and Bobée B. (1999). Une approche pour la sélection des distributions statistiques: application au bassin hydrographique du Saguenay-Lac St-Jean. *Canadian Journal of Civil Engineering*, 26(2), 216-225.

**36.** LeBartier E. and Mary-Huard T. (2004). Le critère BIC: fondements théoriques et interprétation. Rapport de recherche. Institut National de la Recherche en Information et en Automatique (France).16.

**37.** Stedinger J.R., Vogel R.M. and Foufoula-Georgiou E. (1993). Frequency analysis of extreme events. Ch. 18 in: *Handbook of Hydrology* (ed. by D. R. Maidment), McGraw-Hill.New York. USA.

**38.** Réméniéras G. (1972). L'Hydrologie de l'Ingénieur (troisième édn). Collection du Centre de Recherches et d'Essais de Chatou. Eyrolles. France.

**39.** Meylan P., Favre A.C. and Musy A. (2008). Hydrologie fréquentielle: une science prédictive. PPUR presses polytechniques.

**40.** Bertrand-Krajewski J.L. (2007). Stormwater pollutant loads modelling: epistemological aspects and case studies on the influence of field data sets on calibration and verification. *Water Science and Technology*, 55(4), 1-17.

**41.** Musy A.N.D.R.É. (2005). Cours" Hydrologie générale". *Ecole polytechnique fédérale de Lausanne*.

**42.** Benabdesselam T. and Hammar Y. (2009). Estimation De La Réponse Hydrologique D'un Bassin Versant Urbanisé. *European Journal of Scientific Research*, 29(3), 334-348.

**43.** Soro G.E., Goula Bi T.A., Kouassi F.W., Koffi K., Kamagate B., Doumouya I., Savane I. and Srohorou B. (2008). Courbes Intensité Durée Fréquence des précipitations En climat Tropical Humide: Cas de la Région d'Abidjan (Côte D'Ivoire). *European Journal of Scientific Research,* 21(3), 394-405.

**44.** Ague A. and Afouda A. (2015). Analyse fréquentielle et nouvelle cartographie des maxima annuels de pluies journalières au Bénin. *Int. J. Biol. Chem. Sci*., 9(1), 121-133.

**45.** Ferro V., Porto P. and Yu B. (1999). A comparative study of rainfall erosivity estimation for southern Italy and southeastern Australia. *Hydrological Sciences Journal*, 44(1), 3-24.

**46.** Koutsoyiannis D. and Baloutsos G. (2000). Analysis of a long record of annual maximum rainfall in Athens. Greece and design rainfall inferences. *Natural Hazards (Dordrecht),* 22(1), 29-48.

**47.** Pereyra-Díaz D., Pérez-Sesma J.A. and Gómez-Romero L. (2004). Ecuacionesque estiman las curvasintensidad-duración-período de retorno de la lluvia. *Geos*, 24, 46-56.

**48.** Benlaoukli B. and Touaïbia B. (2004). L'expérience algérienne dans le domaine des études de retenues collinaires. *Revue des sciences de l'eau/Journal of Water Science*, 17(2), 153-162.

**49.** Bacro J.N. and Chaouche A. (2006). Incertitude d'estimation des pluies extrêmes du pourtour méditerranéen: illustration par les données de Marseille. *Hydrological sciences journal*, 51(3), 389-405.

**50.** Benabdesselam T. and Hammar Y. (2009). Estimation de la réponse hydrologique d'un bassin versant urbanisé. *European Journal of Scientific Research*, 29(3), 334-348.

**51.** Desbordes M. and Bouvier C. (1990). Assainissement pluvial urbain en Afrique de l'ouest. Modélisation du ruissellement. Rapport final, 408.